ACTA MECHANICA SINICA, Vol.9, No.3, August 1993 ISSN 0567-7718
Science Press, Beijing, China
Allerton Press, INC., New York, U.S.A.

THREE-DIMENSIONAL EVOLUTION OF VORTICES AND EARLY FEATURES OF COHERENT STRUCTURE IN THE TURBULENT WAKE BEHIND A 2-D CIRCULAR CYLINDER*

Ling Guocan (凌国灿) Wu Zuobing (武作兵)[1)]
(*LNM, Institute of Mechanics, Chinese Academy of Sciences Beijing* 100080, *China*)

ABSTRACT: 3-D evolution of Kármán vortex filaments and vortex filaments in braid regions in the turbulent wake of a 2-D circular cylinder is investigated numerically based on inviscid vortex dynamics by analyzing the response of the initially 2-D spanwise vortex filaments to periodic spanwise disturbance of varying magnitude, wavelength and initial phase angles. Our results reveal a kind of 3-D vortex system in the wake which consists of large scale horseshoe-shaped vortices and small scale λ-shaped vortex filaments as well as vortex loops. The mechanism and the dynamic process about the generation of streamwise vortical structure and the 3-D coherent structure are reported.

KEY WORDS: three-dimensional evolution, coherent structure, wake flow

I. INTRODUCTION

It is well known that the wake flows of 2-D bluff body at moderate and high Reynolds numbers can exhibit a 3-D vortical structure. The study of the instability mechanism resulting in these structures is now of special interest which will lead to a better understanding of flow transition in the wake from laminar to turbulent. Early studies are mainly about the vortical structure of large scale such as "vortex pair eddies" or "double roller eddies" (Townsend[1-2], Grant[3], Perge & Lumley[4] and others) in the wake of a circular cylinder. Recent experiments (Shirakashi et al[5], Yamane et al[6]) have shown a new coherent structure—spoon-shaped vortices in the turbulent wake of a circular cylinder, and illustrated the process of reorganization of Kármán vortices resulting in the coherent structure. Williamson[7] discovered a combination structure consisting of deformed primary vortices and finescale streamwise structure. The result indicated another mechanism of formation of 3-D vortical structure, i,e., the 3-D deformation of initially spanwise Kármán vortices and the stretch of vortex filaments in braid regions. Due to the complexity of the 3-D evolution of separated wake, up to now a complete understanding of the whole picture of coherent

Received 20 July 1992, revised 1 April 1993, and currently published in the Chinese Edition of Acta Mechanica Sinica, Vol.25, No.3, 1993
*The project supported by National Natural Science Foundation of China and the National Basic Research Project "Nonlinear Science"
1)Present address: Institute of Theoretical Physics, Chinese Academy of Sciences, Beijing 100080, China

vortical structure and the mechanism has not yet been reached, even in the case where the near wake and intermediate wake are concerned.

As the numerical study on the problem is concerned, most of previous results were about 2-D and 3-D evolution of mixing layer or plane shear layer (Ashurst & Meiburg[8], Meiburg & Lasheras[9], Lasheras & Meiburg[10] and others). Only a few were about the evolution of bluff body wake flows. Okubo et al[11] reported numerical tracing of the deformation process of a single vortex filament of Kármán vortices by applying Aref and Flinchem's[12] method to the wake behind a circular cylinder and confirmed the generation process of the 3-D spoon-shaped vortices. However the numerical model only dealt with a single vortex filament in vortex street, more vortex filaments and the effect from different base flow fields in the wake had not been taken into account. No different scale vortex structures have been found. On the other hand, many previous numerical simulations have demonstrated that the inviscid vortex dynamics may be a reliable modeling technique of the 3-D evolutions of plane shear layers and wake flows especially for simulation of early time evolution.

In the present paper the onset and development of 3-D flow structure in the wake of a circular cylinder will be investigated numerically using inviscid vortex dynamics by analyzing the response of the initially 2-D spanwise vortex filaments in different wake flow fields to periodic spanwise disturbance of varying magnitude and wavelength as well as initial disturbance angles. The mechanism, process and early features of 3-D vortex structure are reported. In the study more vortex filaments and their interaction are considered.

II. METHOD

2.1 Basic Assumptions

(1) An initially 2-D Karman vortex street behind a circular cylinder in uniform flow is considered. Boundary effect is omitted. The 3-D transition of Kármán vortex filaments and vortex filaments in braid regions is studied.

(2) The process of 3-D evolution is traced numerically after the initial spanwise Kármán vortex filaments have broken into several stable vortex segments. The time-averaged velocity profiles in the wake are similar.

(3) The important features of the initial transition process can be reproduced by numerical simulation based on inviscid vortex dynamics. Vortex filaments are thin. The self-induced velocity can be determined by localized induction approximation (LIA) method.

The movement of a vortex filament can be calculated by

$$\frac{\partial \boldsymbol{x}}{\partial t} = \boldsymbol{V}_s(\boldsymbol{x}, t) + \boldsymbol{V}_b(\boldsymbol{x}) \tag{1}$$

where $\boldsymbol{x}$ is the vector of the vortex filament position, $\boldsymbol{V}_s, \boldsymbol{V}_b$ are self-induced velocity and base flow velocity, respectively.

The velocity $\boldsymbol{V}$ at a point $\boldsymbol{x}$ induced by the vortex filament can be calculated by Biot-Savart law, i.e.

$$\boldsymbol{V}(\boldsymbol{x}, t) = -\frac{\Gamma}{4\pi} \int \frac{\boldsymbol{X}' - \boldsymbol{x}}{|\boldsymbol{X}' - \boldsymbol{x}|^3} \times \mathrm{d}\boldsymbol{X}' \tag{2}$$

By the LIA method[12], the self-induced velocity can be simplified as follows

$$\begin{aligned} \boldsymbol{V}_s &= Ck\Gamma \boldsymbol{b} \\ C &= \frac{\pi}{4} \ln(L_\sigma/\sigma) \end{aligned} \tag{3}$$

where Γ is the strength of the vortex, k and $\boldsymbol{b}$ are the local curvature and the binormal unit vector, respectively, L_σ is the cut-off length of the integral interval in Biot-Savart law and σ is the radius of the vortex filament.

2.2 Base Flow Fields

The time-averaged velocity field of the wake and a local flow field near the braid region in Kármán vortex street are considered as two kinds of the base flow field. Using vortex filament dynamics equation, the three dimensional evolution of Kármán vortices and vortex filaments in the braids are studied respectively.

The coordinates are fixed to an undisturbed Kármán vortex, and then the base flow fields can be described as follows.

(1) The time-averaged velocity profile in the wake is:

$$u_b = U_{\max}\{\exp[-\mathrm{y}_s^2/\triangle] - \exp[-\mathrm{y}^2/\triangle]\} \tag{4}$$

where $U_{\max}$ is the maximum defect of the velocity profile and $\triangle$ is a constant parameter which determines the thickness of the shear layer, y_s is a transverse coordinate of Kármán vortex.

(2) The local flow field near the saddle point between two consecutive primary vortices in Kármán vortex street is

$$\begin{aligned} v_{bx} &= \frac{\Gamma}{2\ell}\mathrm{th}(\frac{\pi h}{\ell}) + \frac{\Gamma}{\ell}\frac{\mathrm{ch}(\frac{\pi \mathrm{h}}{\ell})[\cos(\frac{2\pi \mathrm{x}}{\ell})\mathrm{sh}(\frac{2\pi \mathrm{y}}{\ell}) - \mathrm{sh}(\frac{\pi \mathrm{h}}{\ell})]}{[\sin(\frac{2\pi \mathrm{x}}{\ell})\mathrm{ch}(\frac{2\pi \mathrm{y}}{\ell})]^2 + [\cos(\frac{2\pi \mathrm{x}}{\ell})\mathrm{sh}(\frac{2\pi \mathrm{y}}{\ell}) - \mathrm{sh}(\frac{\pi \mathrm{h}}{\ell})]^2} \\ v_{by} &= -\frac{\Gamma}{\ell}\frac{\mathrm{sh}(\frac{\pi \mathrm{h}}{\ell})\sin(\frac{2\pi \mathrm{x}}{\ell})\mathrm{ch}(\frac{2\pi \mathrm{y}}{\ell})}{[\sin(\frac{2\pi \mathrm{x}}{\ell})\mathrm{ch}(\frac{2\pi \mathrm{y}}{\ell})]^2 + [\cos(\frac{2\pi \mathrm{x}}{\ell})\mathrm{sh}(\frac{2\pi \mathrm{y}}{\ell}) - \mathrm{sh}(\frac{\pi \mathrm{h}}{\ell})]^2} \end{aligned} \tag{5}$$

where l and h are the streamwise and transverse spacing of the row of Kármán vortices respectively.

The saddle points are at $A(0, -\frac{1}{2\pi}\ln c)$, $B(\frac{l}{2}, \frac{1}{2\pi}\ln c)$, where

$$c = [\mathrm{ch}(\pi \mathrm{h}/\ell)\sqrt{3 + \mathrm{ch}^2(2\pi \mathrm{h}/\ell)} + 1 + \mathrm{ch}^2(\pi \mathrm{h}/\ell)]/\mathrm{sh}(\pi \mathrm{h}/\ell)$$

2.3 Numerical Method

In the calculation the following non-dimensional quantities denoted by asterisks are introduced:

$$\begin{array}{llll} \boldsymbol{x}^* = \boldsymbol{x}/d & \ell^* = l/d & t^* = t/(\ell/d) & \Gamma^* = \Gamma/(U_\infty d/l) \\ s^* = s/d & \boldsymbol{V}^* = \boldsymbol{V}l/U_\infty d & \Delta^* = \Delta/d & L^* = L/d \end{array} \tag{6}$$

where U_∞ is the uniform flow velocity, d is the diameter of the circular cylinder, l is the streamwise spacing of Kármán vortices.

Using Eqs.(6) and (3), the vortex filament movement expressed by Eq.(1) can be represented as

$$\frac{\partial \boldsymbol{x}^*}{\partial t^*} = C\Gamma^*\frac{\partial \boldsymbol{x}^*}{\partial s^*} \times \frac{\partial^2 \boldsymbol{x}^*}{\partial s^{*2}} + \boldsymbol{v}_b^*(\boldsymbol{x}^*) \tag{7}$$

From now on, the asterisks "*" for the nondimensional quantities are omitted for convenience.

The deformation of the vortex filament is assumed to be periodic along the spanwise direction with a period L, and the periodic boundary condition is imposed in the calculation:

$$\boldsymbol{X}(x,\ y,\ z+L,\ t) = \boldsymbol{X}(x,\ y,\ z,\ t) + L\boldsymbol{k} \tag{8}$$

The vortex filament is subject to an initial exponential or a harmonic disturbance in a spanwise period. That is:

$$\begin{aligned} x &= \varepsilon \cos\theta\ \exp(-z^2/\delta) \\ y &= \varepsilon \sin\theta\ \exp(-z^2/\delta) \end{aligned} \tag{9a}$$

or

$$\begin{aligned} x &= \varepsilon \cos\theta \cos(2\pi z/L) \\ y &= \varepsilon \sin\theta \cos(2\pi z/L) \end{aligned} \tag{9b}$$

where $\theta = 0,\ \pi/2,\ \pi,\ 3\pi/2,\ \theta$ is the angle between the plane of the filament and the x-z plane. ε and δ are constant parameters which prescribe the initial shape of the filament.

The initial width of the filament is given by $Z_w = 2[-\delta\log(0.01)]^{1/2}$, so that the amplitude of initial disturbance at $Z = \pm Z_w/2$ is $1\%\varepsilon$.

Using unequispaced finite difference scheme to discrete the first term of the right-hand side of the Eq.(7)

$$\frac{\partial \boldsymbol{x}_k}{\partial s} \times \frac{\partial^2 \boldsymbol{x}_k}{\partial s^2} = \frac{2\left[\boldsymbol{x}_{k+1}\times\boldsymbol{x}_{k-1} + \boldsymbol{x}_k\times\boldsymbol{x}_{k+1} + \boldsymbol{x}_{k-1}\times\boldsymbol{x}_k\right]}{h_k h_{k+1}(h_k + h_{k+1})} + O(h_k h_{k+1}) \tag{10}$$

where $h_k = \left|\boldsymbol{x}_k - \boldsymbol{x}_{k-1}\right|$.

Using a third order spline representation to calculate approximately the unit tangential vector of vortex filament when Biot-Savart equation is integrated in the space.

The ordinary differential equations which are valid at each discrete point on the filament are obtained

$$\begin{aligned} &\frac{\mathrm{d}\boldsymbol{x}_k}{\mathrm{d}t} = F(\boldsymbol{x}_{k-1},\ \boldsymbol{x}_k,\ \boldsymbol{x}_{k+1}) \\ &F(\boldsymbol{x}_{k-1},\ \boldsymbol{x}_k,\ \boldsymbol{x}_{k+1}) = \frac{2\left[\boldsymbol{x}_{k+1}\times\boldsymbol{x}_{k-1} + \boldsymbol{x}_k\times\boldsymbol{x}_{k+1} + \boldsymbol{x}_{k-1}\times\boldsymbol{x}_k\right]}{h_k h_{k+1}(h_k + h_{k+1})} + \boldsymbol{v}_2(\boldsymbol{x}_k) \end{aligned} \tag{11}$$

The fourth order Runge-Kutta method with the variable stepsize is employed in the time integration of Eq.(11), then we have

$$\begin{aligned} &\boldsymbol{x}_k(t+\Delta t) = \boldsymbol{x}_k(t) + (\Delta'\boldsymbol{x}_k + 2\Delta''\boldsymbol{x}_k + 2\Delta'''\boldsymbol{x}_k + \Delta''''\boldsymbol{x}_k)/6 \\ &\Delta'\boldsymbol{x}_k = \Delta t F(\boldsymbol{x}_{k-1},\ \boldsymbol{x}_k,\ \boldsymbol{x}_{k+1}) \\ &\Delta''\boldsymbol{x}_k = \Delta t F(\boldsymbol{x}_{k-1} + 0.5\Delta'\boldsymbol{x}_{k-1},\ \boldsymbol{x}_k + 0.5\Delta'\boldsymbol{x}_k,\ \boldsymbol{x}_{k+1} + 0.5\Delta'\boldsymbol{x}_{k+1}) \\ &\Delta'''\boldsymbol{x}_k = \Delta t F(\boldsymbol{x}_{k-1} + 0.5\Delta''\boldsymbol{x}_{k-1},\ \boldsymbol{x}_k + 0.5\Delta''\boldsymbol{x}_k,\ \boldsymbol{x}_{k+1} + 0.5\Delta''\boldsymbol{x}_{k+1}) \\ &\Delta''''\boldsymbol{x}_k = \Delta t F(\boldsymbol{x}_{k-1} + 0.5\Delta'''\boldsymbol{x}_{k-1},\ \boldsymbol{x}_k + 0.5\Delta'''\boldsymbol{x}_k,\ \boldsymbol{x}_{k+1} + 0.5\Delta'''\boldsymbol{x}_{k+1}) \end{aligned} \tag{12}$$

In the calculation the parameters used are: $\Gamma = 2.265,\ l = 5.47,\ h = 1.66,\ c = 0.111,\ \varepsilon = 0.02,\ Z_w = 2$, which are similar to those used by Okubo et al[11]. For Γ is chosen in the typical Kármán vortex street, so $U_{\max}$ and Δ are chosen at an appropriate location:

$U_\infty = 1.337$ and $\Delta = 1.332$. Shirakashi et al[5] and Yamane et al[6] have reported that the spanwise Kármán vortex filament is firstly broken into length of $8d$ in the process of evolution to a three-dimensional large scale structure, so the spanwise wave length $L = 8$ is considered. From Okubo & Matsui[13] and Okubo et al[14] the vorticity at the saddle point can be estimated approximately, which is 5% of vorticity at the vortex center, so the circulation Γ' at the saddle point is approximately 5% of the circulation Γ of a Kármán vortex. Considering symmetry about the x-y plane the deformation of vortices is calculated only for $Z \geq 0$. The number of node points N and the accuracy ΔE of the calculation are chosen as $N = 200$, $\Delta E = 0.0001$ respectively. When more vortex filaments' interaction is considered, the number of node points is reduced to $N = 20$.

IV. NUMERICAL RESULTS

4.1 3-D Evolution of Single Vortex Filament of Kármán Vortices

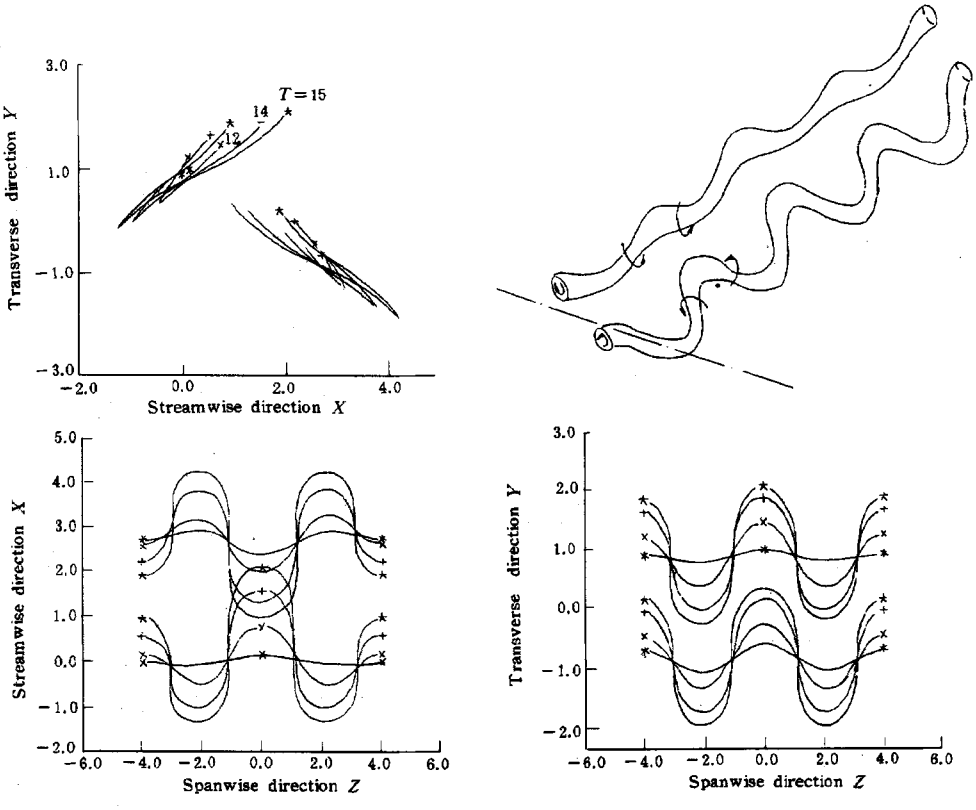

Fig.1 3-D evolution of Kàrmàn vortices and formation of "horseshoe" vortices
— * — T=10 — × — T=12 — + — T=14 — ⋆ — T=15
initial angle=90°

The calculated results show that the Kármán vortex and the vortex filament in the braid region of wake flow have spanwise instability. Through the interaction between the self-induction and the shear base flow, the initially spanwise Kármán vortex in the time-averaged velocity field evolves into a 3-D configuration like a horseshoe-shaped vortex in an inclined plane. As time goes on the upper and lower horseshoe vortices lie respectively on planes of approximately 45° and 135° to the x-z plane (x and z are streamwise and spanwise

direction respectively). The final spanwise scale of the deformed region of the filament has an almost constant value of $4d$. Fig.1 shows some samples of calculated results on the evolution with time of vortex filaments, the initial disturbance phase angle $\theta = 90°$. The time step used is 0.001. It shows the amplitude of wavy vortex increases rapidly with time, and the vortex turns its direction generating the streamwise vorticity and is stretched. Later on, the inclination angles of upper and lower vortices almost reach constant values of 45° and 135°. The two wavy vortices are 180° out of phase in the spanwise direction in x-z plane. Fig.2

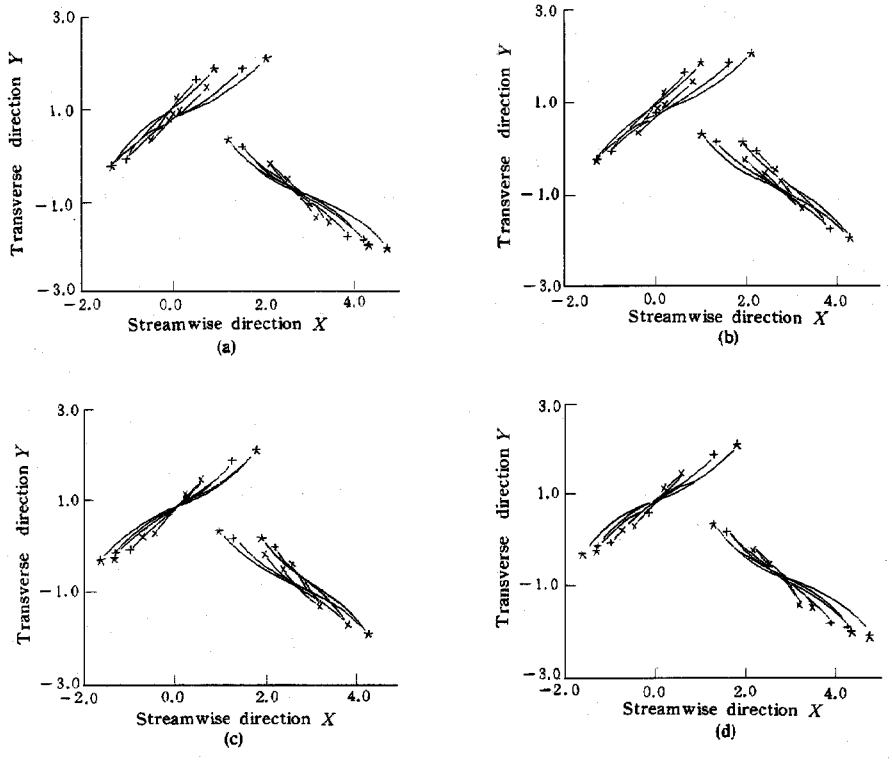

Fig.2 The side view of the evolution of Kármán vortices
— * — T=10 — × — T=12 — + — T=14 — ⋆ — T=15
initial angle: (a) 0° (b) 90° (c) 180° (d) 270°

shows the side-view (streamwise-transverse x-y plane) results of vortex evolution for different initial phase angles $\theta = 0°, 90°, 180°$ and 270° respectively. It is clear that all evolved Kármán vortices finally assume the structures lying on the planes of nearly 45° and 135° with respect to x-z plane irrespective to the orientation of the initial disturbance, and the upper and lower vortices are wavy in phase each other for the cases of $\theta = 0°$ and 180°. The spanwise scale of these deformed vortex structure is nearly the same.

These calculated results are comparable to some previous studies. For instance, Hussain & Hayakawa[15] indicated that Kármán vortices may evolve into two possible configurations of the horseshoe-like structure. Okubo et al[11] indicated that the inclined angle of the deformed vortex was 30°∼40°. Mumford[16] mentioned the angle of 45° as a typical value of the roller eddies. Bonnet et al[17] and Hayakawa & Hussain[18] obtained a 60° inclination angle of an organized structure. The final spanwise scale of the deformed region of the filament given by Okubo et al[11] is about 4–6d.

4.2 Evolution of Kármán Vortex Calculated Considering More Vortex Filaments

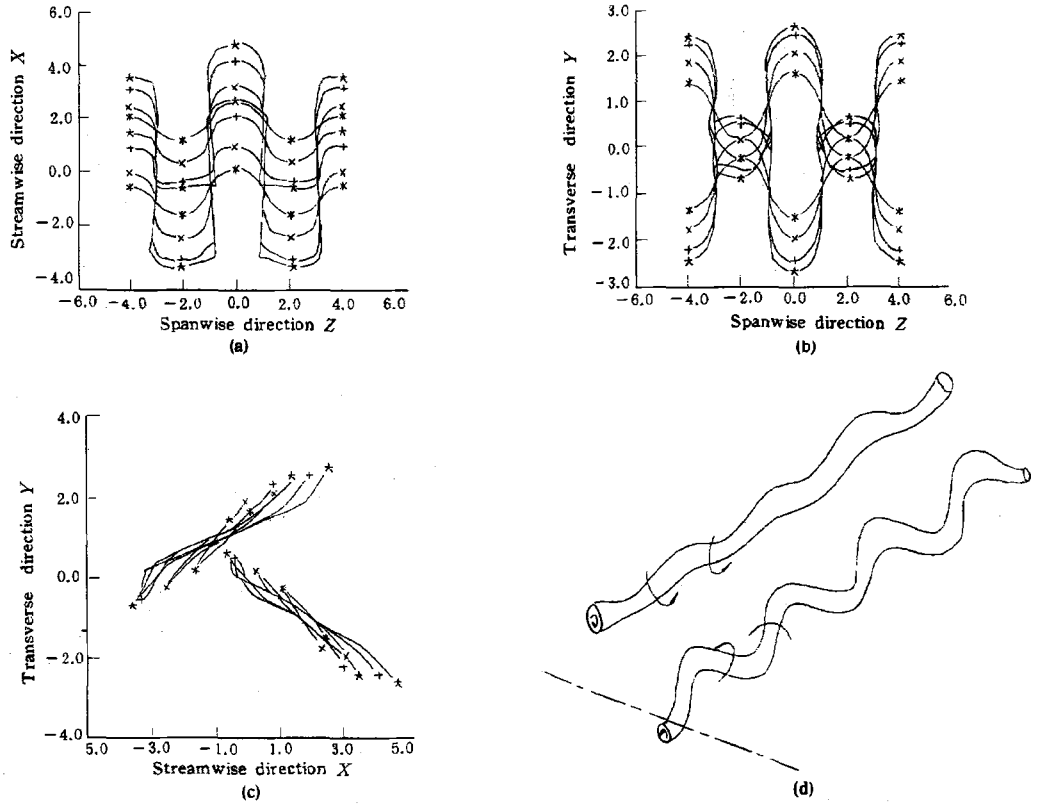

Fig.3 3-D evolution of Kármán vortices, with vortex interaction
— * — T=10 — × — T=12 — + — T=14 — ⋆ — T=15
initial angle=0°

When the interaction of Kármán vortex with its neighbour vortex filaments is taken into account in numerical model, the calculated global features of evolution of the Kármán vortex are very similar to those mentioned above for a single vortex evolution, but the wavy features in x-z plane of upper and lower vortices are almost in phase irrespective to the orientation of the initial small disturbance. Fig.3 gives some examples of the particular evolution process. It shows that the upper and lower Kármán vortices are gradually turning their direction and being stretched. The spanwise instability rapidly grows when the time increases. Later the two deformed vortices are on two planes of approximately 45° and 135° with respect to the x-z plane. The characteristic length in spanwise direction of these deformed vortical structure is $4d$, which is the same as the single vortex deformation. For various phase angles of initial disturbance $\theta(0°, 90°, 180°, 270°)$ calculations yield similar results such as those of the inclined angle of vortices and the spanwise scale of the horseshoe vortices. The in-phase feature of wavy upper and lower vortices is due to the interaction effect among vortex filaments.

4.3 3-D Evolution of Vortex Filament in the Braid Region

A typical calculated results of evolution of vortex filaments subject to the braid region flow field between two consecutive Kármán vortices are shown in Fig.4. These vortex

filaments with less circulation assume a small scale vortical structure. In calculation the

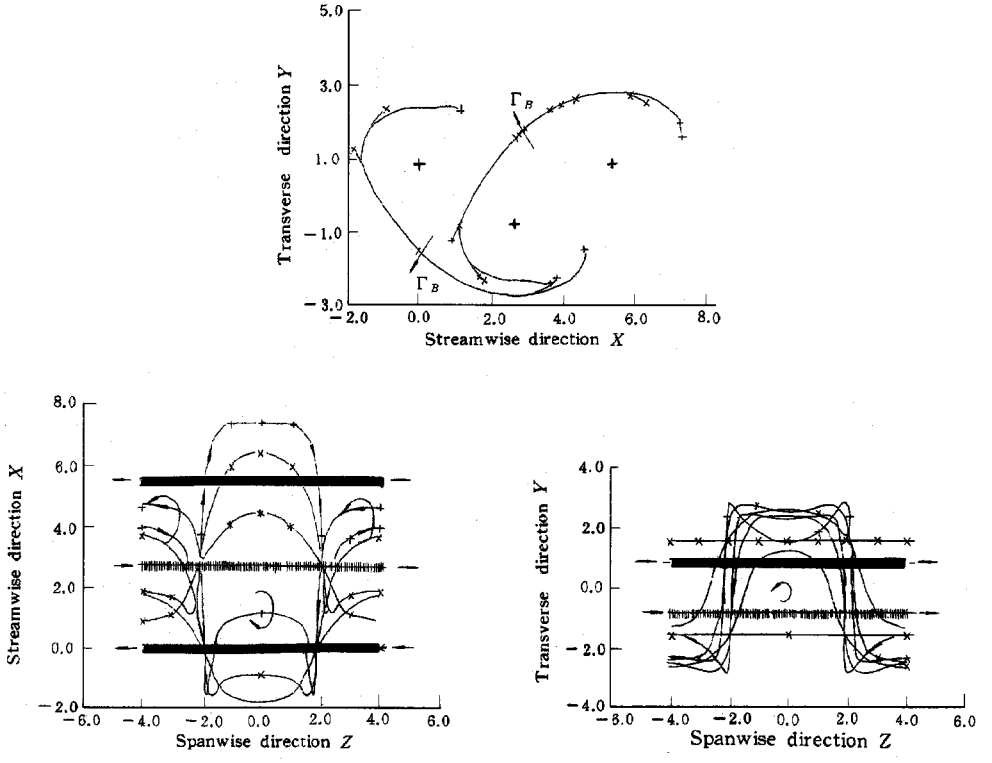

Fig.4 3-D evolution of vortex filaments in the braid regions and formation of closed vortex loops with an asymmetric configuration along the spanwise direction
— * — T=40 — × — T=50 — + — T=60
initial angle=90°

initial time step is 0.02 and $\theta = 90°$. With the time increasing the upper and lower vortex filaments gradually turn to the principal strain planes in the flow field and are very much stretched. Then the two filaments wrap two consecutive Kármán vortices as also shown in Fig.5. The two deformed vortices are 180° out of phase each other in the spanwise direction, and form a vortex pair inclining to the x-z plane, having a nearly λ-shaped configuration viewing from x-y plane along x direction. Thus the two consecutive Kármán vortices with alternating signs and the λ vortices constitute a nearly closed vortex loop. The upper and lower λ-shaped vortices are 180° out of phase each other in the spanwise direction in x-z plane. The nearly closed vortex loop interlocks half of wave length and two consecutive loops form an asymmetric configuration along the spanwise direction. For $\theta = 180°$ (or 0°), the evolution of vortex filaments presents same behavior as that calculated in the case of $\theta = 90°$ (or 270°), but the λ-shaped vortices in two consecutive braids are in phase each other and the formed upper and lower vortex loops have a symmetric configuration. The present results are similar to those of Williamson's[7] observation, i.e. in the wake of circular cylinder a kind of small scale streamwise vortex filaments, connect with the large scale deformed Kármán vortex filaments to form the closed vortex loops. Some results given by Meiburg & Lasheras[9] have shown that depending on the oreintation of initial disturbance the wake behind a plane plate develops a symmetric or an asymmetric configuration, which is similar to the present results.

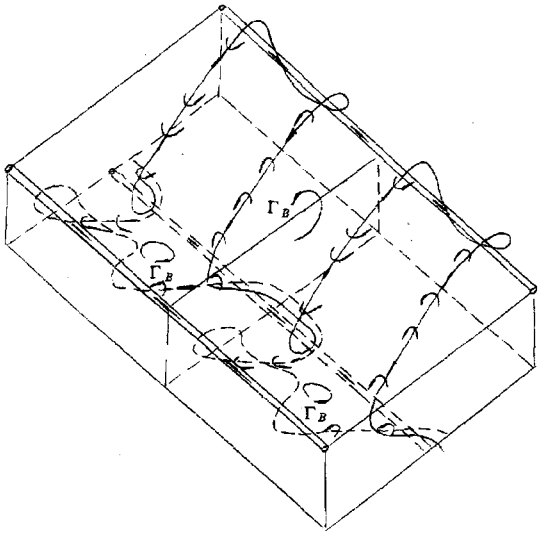

Fig.5

All of our results demonstrate that the deformation and stretching of both Kármán vortices and vortex filaments in braid regions lead to the formation of a 3-D vortex systems which consist of large scale horseshoe vortices and small scale λ-shaped vortex filaments.

V. CONCLUSIONS

1. The calculated results reveal the temporal and spatial process for the reorientation and the redistribution of the initial spanwise vorticity resulting in streamwise vorticity.
2. Our results demonstrate that the mechanism and dynamic process of the 3-D transition can be explained by the deformation and stretching of Kármán vortices and the vortex filaments in the braid regions in the two dimensional vortex shedding model.
3. Present study exhibits the early features of coherent structure in wake development, it is described as a three-dimensional vortex system, which consists of large scale horseshoe-shaped vortices and small scale λ-shaped vortex filaments as well as their combinations-three dimensional vortex loops.
4. The calculated global features of the structure are not related to the orientation of the initial small disturbance.
5. The mechanism of the formation of 3-D structure based on the present results is rather different from the assumption that the structure is formed only by deformation of Kàrmàn vortices proposed by Okubo et al[11]. However the present results are, in some aspects, in agreement with some previous experimental flow visualizations.

REFERENCES

[1] Townsend AA. The Structure of Turbulent Shear Flow. Cambridge: Cambridge University Press. 1956
[2] Townsend AA. *J Fluid Mech*, 1979, 95: 515
[3] Grant ML. *J Fluid Mech*, 1958, 4: 149
[4] Perge F and Lumley J. *Phys Fluids Supp*, 1967, 10: S194.
[5] Shirakashi M, Yamaguchi S, Mochimaru Y and Yamane R. *Fluid Dyn Res*, 1988, 4: 25
[6] Yamane R, Tanaka H, Mochimaru Y, Yagita M and Shirakashi M. *Bell JSME*, 1986, 29-257, 3767

[7] Williamson CHK. *Phys Fluids*, 1988, b, 31: 3165
[8] Ashurst MT and Meiburg E. *J Fluid Mech*, 1988, 189: 87
[9] Meiburg E and Lasheras J. *J Fluid Mech*, 1988, 190: 1
[10] Lasheras JC and Meiburg E. *Phys Fluids*, 1990, 34: 371
[11] Okubo M, Yamane R and Oshima S. *Fluid Dyn Res*, 1988, 4: 39
[12] Aref H and Flinchem EP. *J Fluid Mech*, 1984, 148: 477
[13] Okubo M and Matsui T. *Trans Japan Soc Aero Space Sci*, 1990, 33(99): 1
[14] Okubo M and Matsui T. *J Japan Sco Fluid Mech*, 1991, 10, 24(in Japanese)
[15] Hussain AKMF and Hayakawa M. *J Fluid Mech*, 1987, 180: 193
[16] Mumford JC. *J Fluid Mech*, 1983, 137: 447
[17] Bonnet JP, Delville J and Garem H. *Exp Fluids*, 1986, 4: 189
[18] Hayakawa M and Hussain AKMF. *J Fluid Mech*, 1989, 206: 375